Supplementary Material (ESI) for Chemical Communications

Lanthanide luminescent anion sensing: evidence of multiple anion recognition through hydrogen bonding and metal ion coordination

Cidália M. G. dos Santos, Pablo Barrio Fernández, Sally E. Plush, Joseph P. Leonard, and Thorfinnur Gunnlaugsson*

Electronic Supplementary Information

Synthesis

2-{4,7-bis-dimethylcarbamoylmethyl-10-[(4-nitro-phenylcarbamoyl)-methyl]-1,4,7,10-tetraaza-cyclododec-1-yl}-*N,N*-dimethyl-acetamide (4)

To a solution of **2** (0.282 g, 0.659 mmol) and **3** (0.156g, 0.725 mmol) in MeCN (20 mL) was added potassium iodide (0.121 g, 0.725 mmol) and caesium carbonate (0.236 g, 0.725 mmol). The reaction mixture was then refluxed under an argon atmosphere for 72 hours. The brown solution was filtered through celite and the solvent was removed under reduced pressure. The compound was purified by alumina column chromatography under gradient elution conditions (DCM - MeOH) to give the desired product, **4**, as a brown solid (0.297 g, 74 % yield). m.p. 79-80˚C; m/z 606.37 (M + H), 628.35 (M + Na); Calculated for $C_{28}H_{48}N_9O_6$ [M+H peak] m/z = 606.3734. Found m/z = 606.3728; δ_H(400 MHz, $CDCl_3$) 11.26 (broad s, 1H, NH), 8.17 (d, 2H, ArCH, *J* = 9.36 Hz), 8. 05 (d, 2H, ArCH, *J* = 9.36 Hz), 3.71 (s, 2H, CH_2), 3.5 – 2.0 (m, m, $CH_2CONCH3$ + CH_2 cyclen); δ_C (100 MHz, $CDCl_3$) 171.81, 170.41, 170.21, 145.21, 142.11, 123.87, 119.04, 57.15, 54.64, 54.50, 53.04, 49.72, 35.75, 35.63, 35.22, 35.13.

2-{4[(4-amino-phenylcarbamoyl)-methyl]-7,10-bis-dimethylcarbamoylmethyl-1,4,7,10-tetraaza-cyclododec-1-yl)}-*N,N*-dimethyl-acetamide (5)

To a stirring solution of **4** (0.078 g, 0.129 mmol) and 10 % Pd/C catalyst in EtOH (3 mL), a solution of hydrazine monohydrate (0.052 g, 1.032 mmol) in EtOH (5 mL) was added dropwise. The reaction mixture was then heated under reflux overnight, under an argon atmosphere. The brown solution was filtered through celite and the solvent was removed under reduced pressure to yield the product **5**, as a brown resin (0.065 g, 88 % yield). m/z

508.38 (M + Na); Calculated for $C_{28}H_{49}N_9O_4Na$ [M+Na peak] m/z = 598.3805. Found m/z = 598.3830; δ_H(400 MHz, $CDCl_3$) 10.07 (broad s, 1H, NH), 7.57 (d, 2H, ArCH, *J* = 8 Hz), 6.54 (d, 2H, ArCH, *J* = 8.56 Hz), 3.4 – 2.4 (m, $CH_2CONCH3$ + CH_2 cyclen); δ_C (100 MHz, $CDCl_3$) 170.97, 170.72, 169.80, 142.55, 130.74, 121.15, 114.93, 57.99, 54.95, 53.46, 52.42, 50.90, 36.25, 36.09, 35.65, 35.53.

2-(4,7-Bis-dimethylcarbamoylmethyl-10-{[4-(3-p-tolyl-ureido)-phenylcarbamoyl]-methyl}-1,4,7,10-tetraaza-cyclododec-1-yl)-*N*,*N*-dimethyl-acetamide (1)

To a solution of **5** (0.15 g, 0.261 mmol) in $CHCl_3$ (7 mL) was added trifluoro-p-tolyl isocyanate (0.049 g, 0.264 mmol). The reaction mixture was left stirring under an argon atmosphere at room temperature overnight. The solvent was removed under reduced pressure to yield a pale brown solid. The compound was purified by alumina column chromatography under gradient elution conditions (DCM - MeOH) to give the desired product **1**, as a yellow solid (0.133 g, 67 % yield). m.p. 187-189˚C; m/z 763.42 (M + H); Calculated for $C_{36}H_{54}N_{10}O_5F_3$ [M+H peak] m/z = 763.4231. Found m/z = 763.4248; δ_H(400 MHz, $CDCl_3$) 10.07 (broad s, 1H, NH), 9.94 (broad s, 1H, NH), 9.48 (broad s, 1H, NH), 7.76 (d, 2H, ArCH, *J* = 8.52 Hz), 7.59 (d, 2H, ArCH, *J* = 8.52 Hz), 7.42 (m, 4H, ArCH), 7.35 (d, 2H ArC<u>H</u>, *J* = 8.2 Hz), 3 – 2 (m, 42H, C<u>H</u>$_2$CONC<u>H</u>$_3$, C<u>H</u>$_2$CONH, and C<u>H</u>$_2$ cyclen); δ_C (100 MHz, $CDCl_3$) 170.47, 170.16, 169.48, 153.08, 143.30, 135.16, 133.13, 125.54, 125.27, 119.67, 118.40, 117.42, 57.50, 54.51, 54.31, 51.52, 50.36, 49.61, 36.04, 35.63, 35.49, 35.19, 35.02; δ_F (376 MHz, $CDCl_3$) -61.88 (CF_3).

Tb(III) complex (1.Tb)

A solution of **1** (0.05 g, 0.066 mmol) and $Tb(CF_3SO_3)_3$ (0.04 g, 0.066 mmol) in MeCN (5 mL) was heated under reflux, under an argon atmosphere for 48 hours. The complex was isolated by precipitation from dry ethyl ether (200 mL) as a pale beige solid (0.067 g, 74 % yield). m/z 460.16 ([(M + H)/2); Calculated for $C_{36}H_{52}N_{10}O_5F_3Tb$ [M peak] m/z = 920.3228. Found m/z = 920.3286 δ_H(400 MHz, CD_3OD) 75.92, 51.76, 47.91, 46.87, 40.93, 26.92, 24.70, 21.16, 11.17, 9.03, 7.29, 5.72; δ_F (376 MHz, CD_3OD) -64.20, -79.85.

Figure 1. ^{1}H NMR of **1** (CDCl3, 400 MHz)

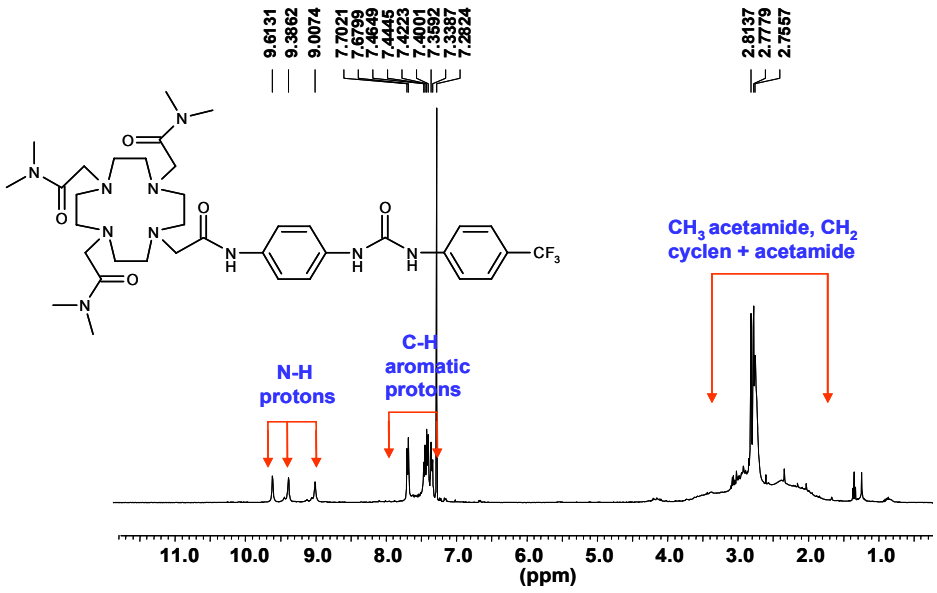

Figure 2. Profile of the absorption changes at 270 nm and at 330 nm, upon gradual additions of $H_2PO_4^-$ (0 – 57.3 µM) in MeCN, versus the number of equivalents of phosphate added.

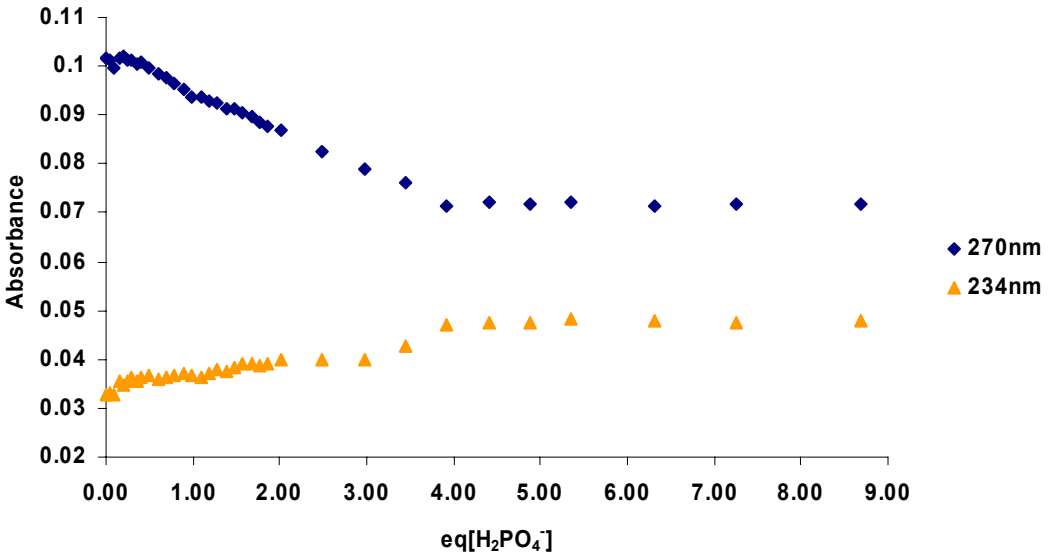

Figure 3. Experimental binding isotherm for the UV-Visible titration of **1.Tb** (4 μM) with $H_2PO_4^-$ in MeCN and corresponding fit from SPECFIT. Data represented by the red circles, while the fit is represented by the solid black line.

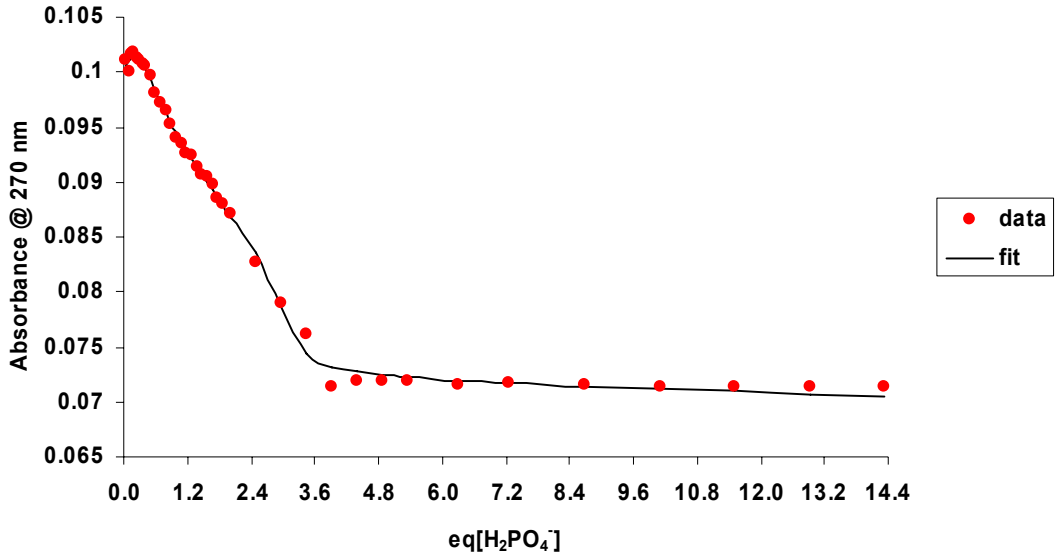

Figure 4. Absorption spectra showing the changes in absorbance of **1.Tb** (4 μM) upon gradual additions of CH_3COO^- (0 – 74.9 μM) in MeCN.

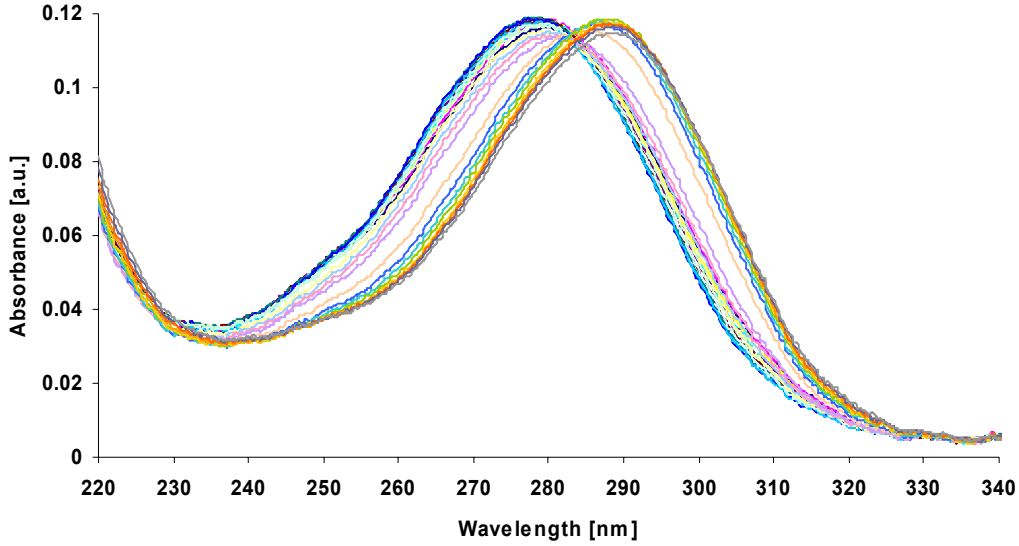

Figure 5. Speciation diagram for the UV-Visible titration of **1.Tb** (4 μM) with CH_3COO^-. Red line refers to the free sensor **1.Tb**, the green line to the complex **CH_3COO^-. 1.Tb** and the pink line to the **$(CH_3COO^-)_2$.1.Tb**.

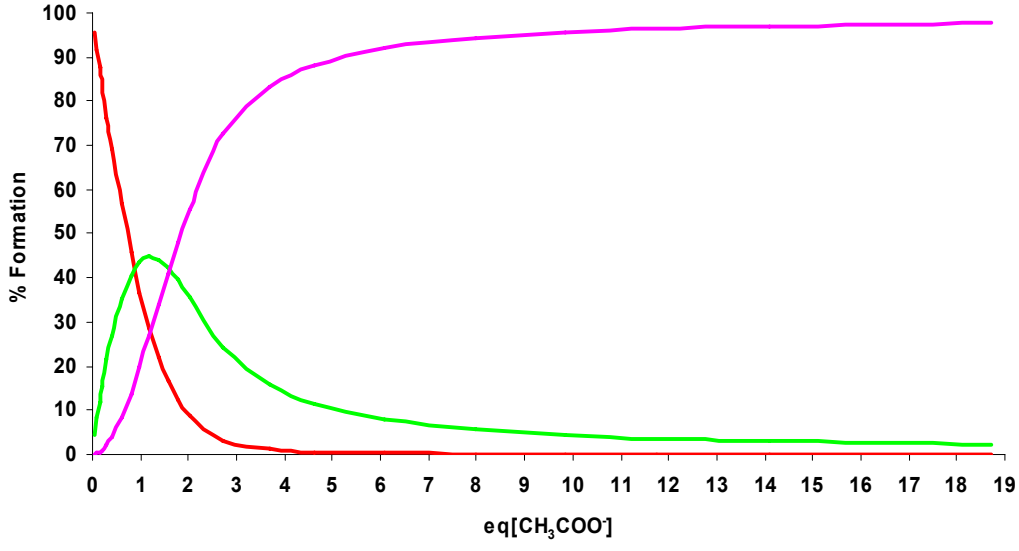

Figure 6. Experimental binding isotherm for the UV-Visible titration of **1.Tb** (4 μM) with F^- in MeCN and corresponding fit from SPECFIT. Data represented by the red circles, while the fit is represented by the solid black line. Binding constants are listed below.

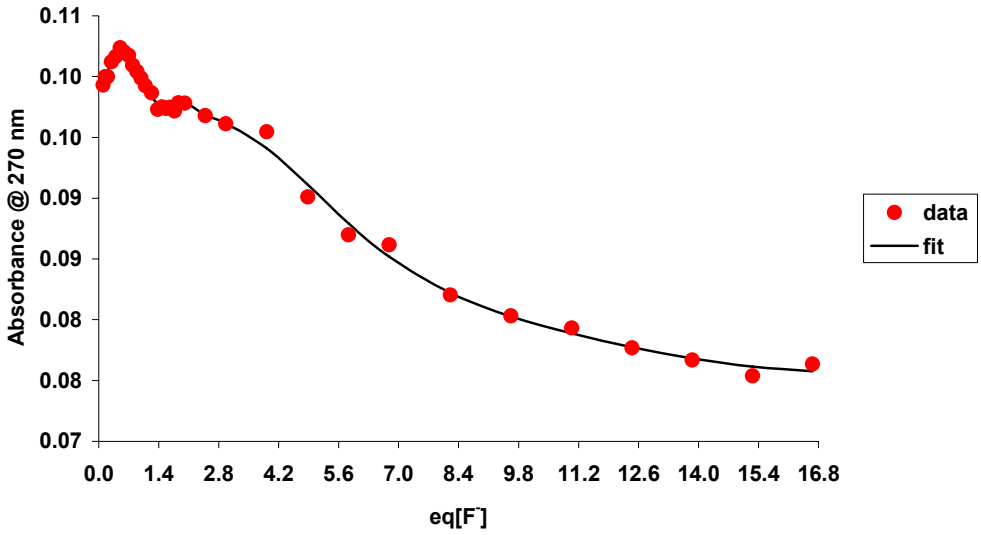

Anion	Technique	Species (G_n:L_m)	Log $\beta_{n:m}$	Std. Deviation
F^-	Absorbance	G:L	5.97	0.181
		$G:L_2$	4.73	0.310*
		G_2:L	5.16	0.162
		$G_2:L_2$	5.52	0.454*
		G_3:L	4.49	0.189
		G_4:L	4.82	0.312
		G_5:L	3.51	0.703*
	Phosphorescence	G:L	6.07#	0.020
		$G:L_2$	4.13#	0.038*
		G_2:L	5.36#	0.014
		$G_2:L_2$	4.47	0.164*
		G_3:L	3.42	0.623*
		G_4:L	6.90	0.011
		G_5:L	2.85	0.773*
	Fluorescence	G:L	6.29	0.114
		$G:L_2$	3.92	0.869*
		G_2:L	5.58	0.247
		$G_2:L_2$	5.11	0.531*
		G_3:L	5.44	0.094
		G_4:L	5.07	0.225
		G_5:L	5.69	0.149

Table 1. Binding constants and binding modes between F^- and sensor **1.Tb**. ***** species present in solution in less than 10% formation. $^{\#}$ represents the values previously found and so considered as fixed values.

Figure 7. Speciation diagram for the UV-Visible titration of the ligand (L) **1.Tb** (4 μM) with F^- in MeCN. Speciation is shown relative to the number of equivalents of F^- (G) added.

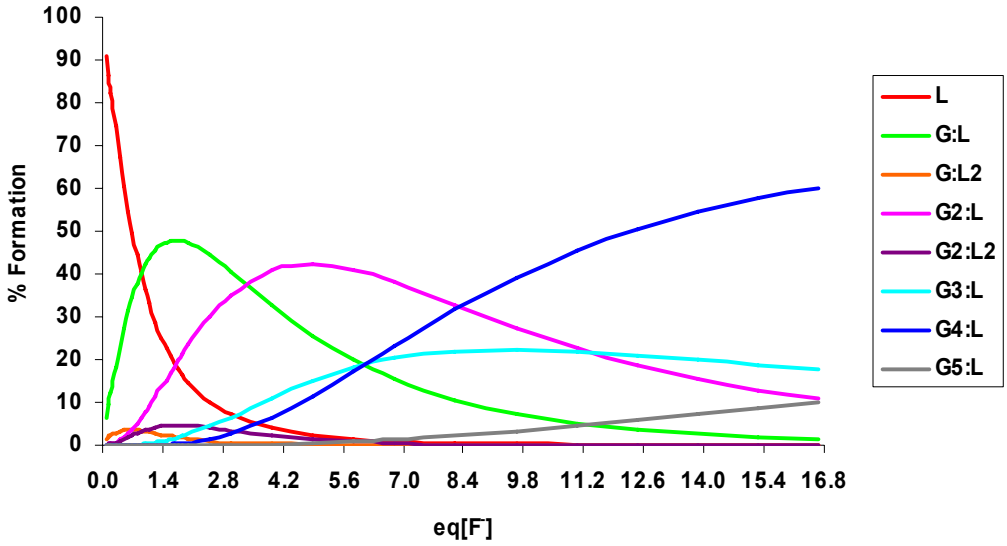

Figure 8. Fluorescence spectra showing the changes in fluorescence intensity of **1.Tb** (4 μM) upon gradual additions of $H_2PO_4^-$ (0 – 57.3 μM) in MeCN, by exciting the sample at 280 nm.

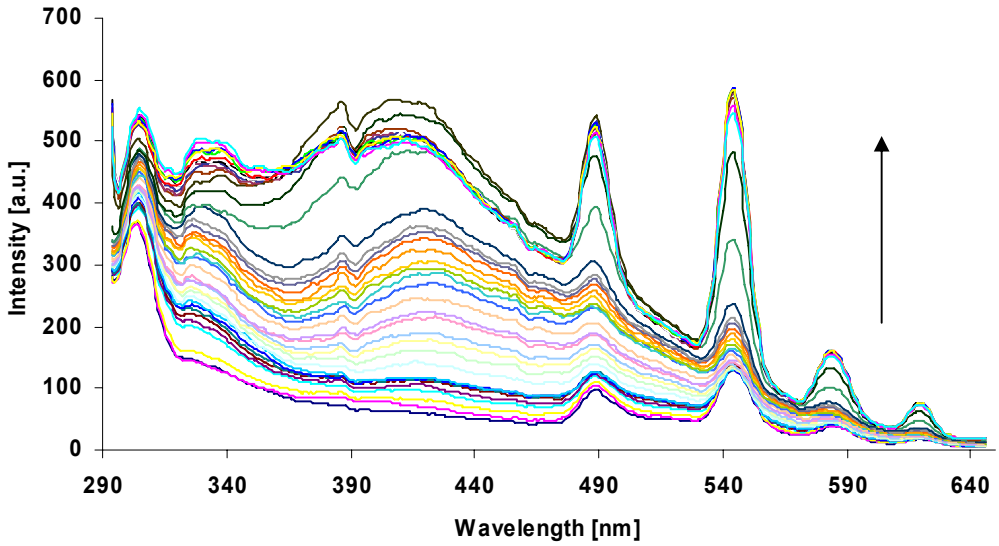

Figure 9. Speciation diagram for the fluorescence luminescence titration of the ligand (L) **1.Tb** (4 μM) with $H_2PO_4^-$ in MeCN. Speciation is shown relative to the number of equivalents of $H_2PO_4^-$ (G) added. Inset showing the experimental binding isotherm and corresponding fit from SPECFIT. Data represented by the green circles, while the fit is represented by the solid black line.

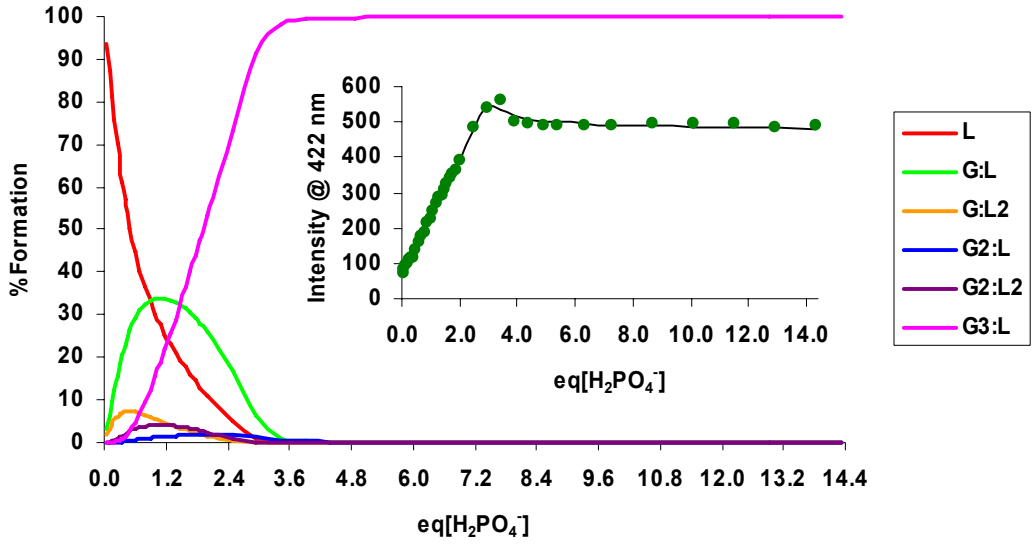

Figure 10. Tb(III) emission spectra showing the changes in emission intensity of **1.Tb** (4 μM) upon gradual additions of CH_3COO^- (0 – 74.9 μM) in MeCN, when using an excitation wavelength of 280 nm.

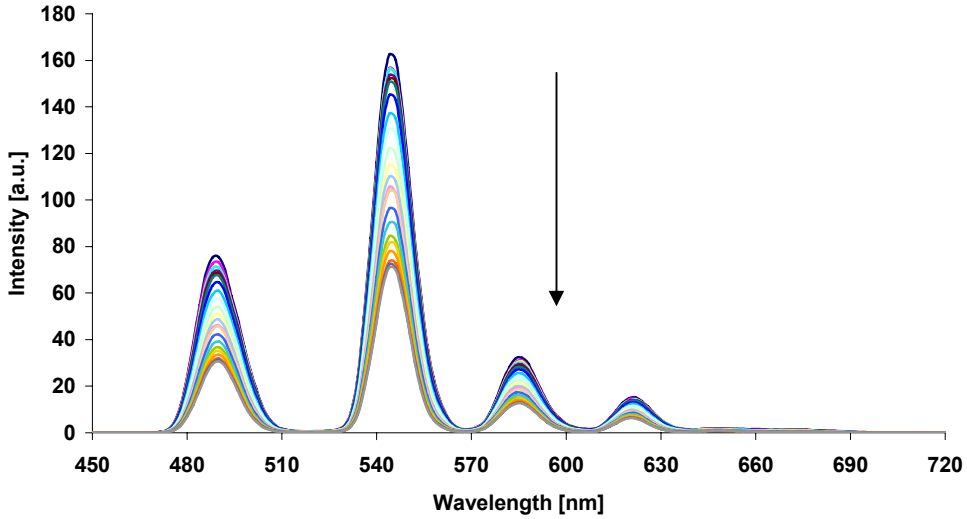

Figure 11. Experimental binding isotherm for the lanthanide luminescence titration of **1.Tb** (4 μM) with CH_3COO^- in MeCN and corresponding fit from SPECFIT. Data represented by the red circles, while the fit is represented by the solid black line.

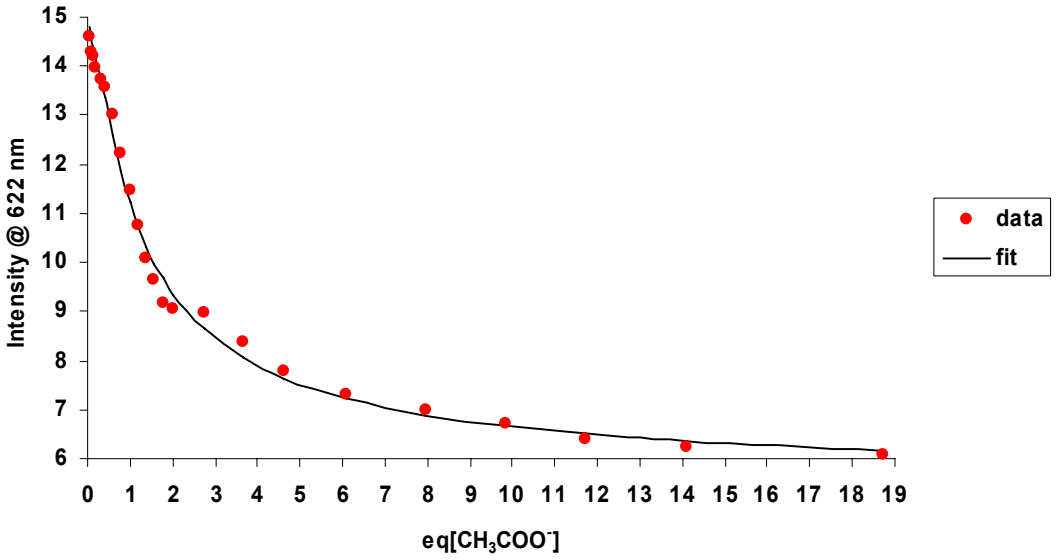

Figure 12. Changes in the Tb(III) emission of **1.Tb** (cs017r0) upon addition of CH_3COO^- in MeCN, followed by the addition of $H_2PO_4^-$

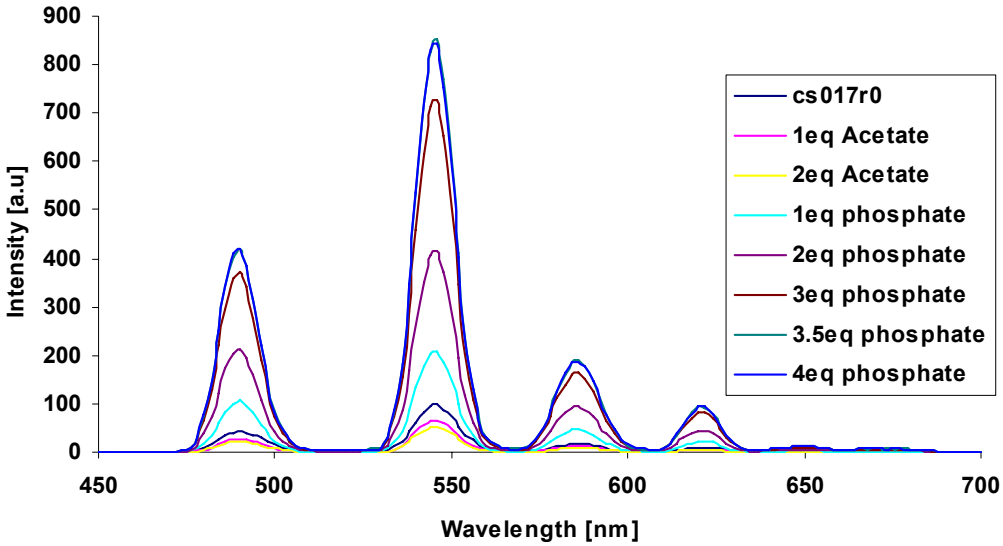

Figure 13. Changes in the absorption spectra of the model compound **7** upon titration gradual additions of $H_2PO_4^-$ (0 – 1.63 mM) in MeCN.

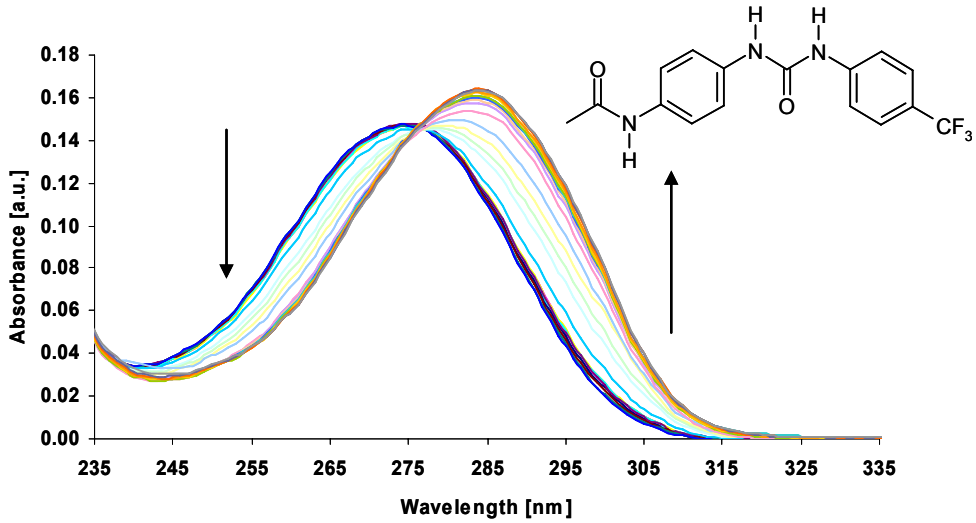

Figure 14. The Experimental binding isotherm for the UV-Visible titration of **7** (4 μM) with $H_2PO_4^-$ in MeCN and corresponding fit from SPECFIT. Data represented by the red circles, while the fit is represented by the solid black line. *Insert*: Speciation diagram for the UV-Visible titration of the model receptor (L) **7** (4 μM) with $H_2PO_4^-$ in MeCN. Speciation is shown relative to the number of equivalents of $H_2PO_4^-$ (G) added.

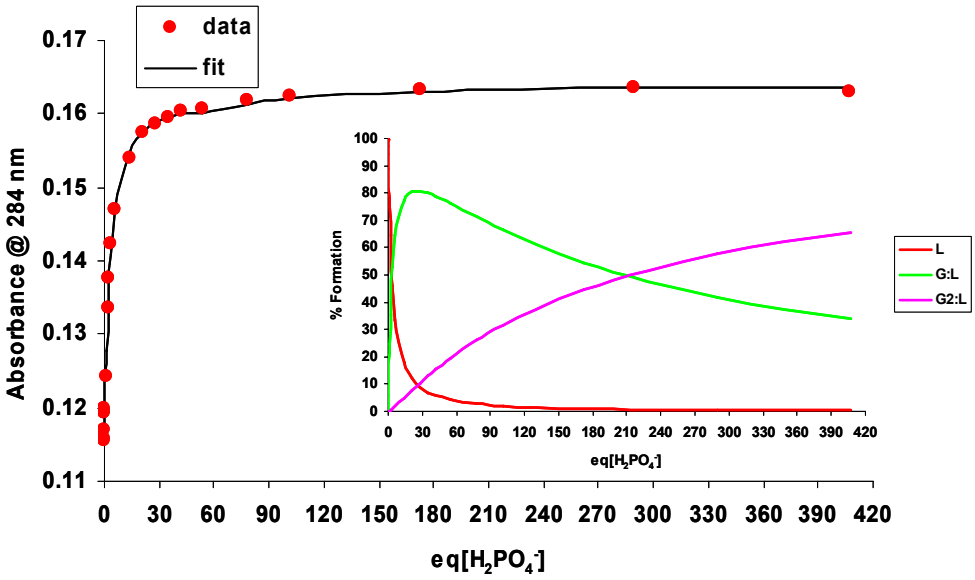

Figure 15. The changes in the lifetimes of the Tb(III) emission upon titration with $H_2PO_4^-$ in MeCN. These results mirror the two step changes observed in the Tb(III) emission densities shown in Figure 3 in the manuscript.

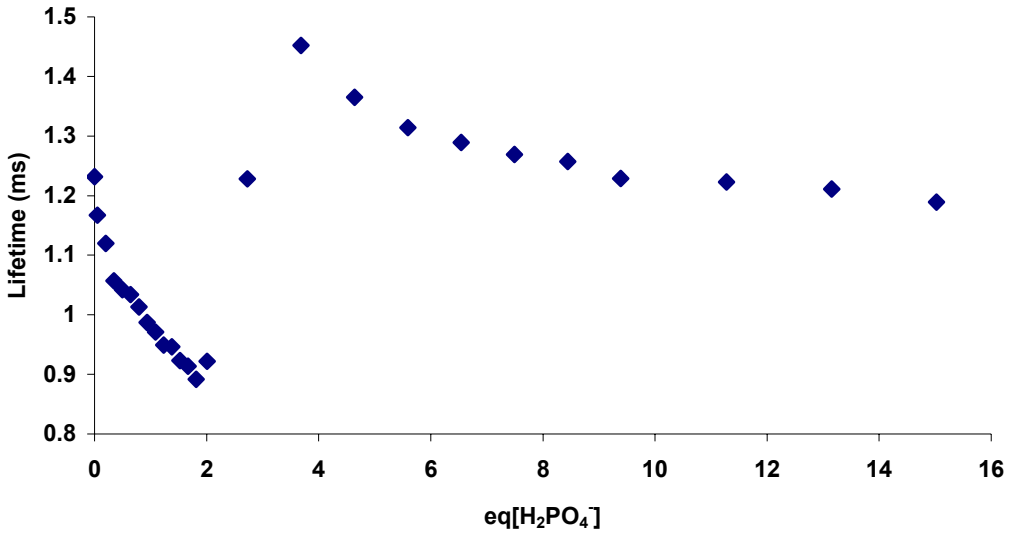

Figure 16. The spectra of the Tb(III) and Eu(III) complexes in MeCN, under the same setting conditions: slits = 10, PMT = 800V, are shown below. This shows that the antenna is able to transfer its energy to the Tb(III) complex, while the Eu(III) emisison is quenched by PET.

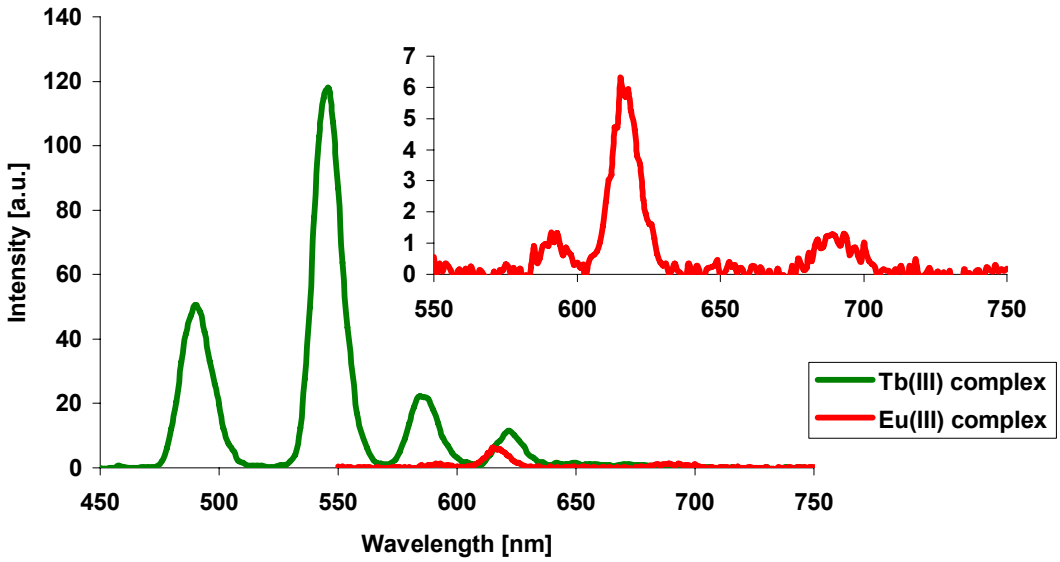

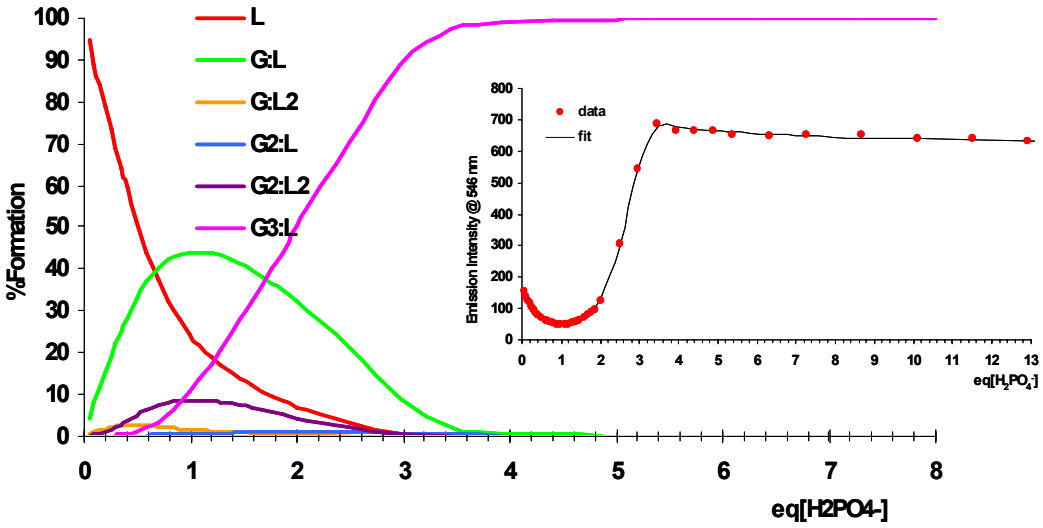

The speciation distribution diagram for the binding of $H_2PO_4^-$ to **1.Tb** for the changes observed for the 546 nm transition. *Insert*: The changes in the Tb(III) emission at 546 nm and the fitted data.